

A Narrowband Photothermoelectric Detector Using Guided-Mode Resonance Filter

Hosein Monshat,¹ Longju Liu,² and Meng Lu^{1,2,*}

¹Department of Mechanical Engineering, Iowa State University, Ames, IA 50011
 Department of Electrical and Computer Engineering, Iowa State University, Ames, IA 50011
 *email: menglu@iastate.edu

Abstract: A narrowband photothermoelectric detector is demonstrated by integrating a guided-mode resonance (GMR) filter and a thin-film thermocouple. The detector utilizes the GMR effect to selectively absorb light at a specific wavelength and raise the temperature at the thermocouple. The voltage output of the thermocouple strongly depends on the coupling between the GMR mode and incoming light. © 2018 The Author(s)

OCIS codes: (130.7408) Wavelength filtering devices, (230.5298) Photonic crystals, (350.5340) Photothermal effects.

The photothermoelectric effect (PTE) is known as the light-induced thermoelectric voltage across a junction between two materials with different Seebeck coefficients [1]. Various PTE-based detectors have been demonstrated in a broad wavelength range, from visible to terahertz [2]. By coupling the broadband PTE detector with a narrowband optical filter, it is possible to design a narrowband PTE detector. Recently, Mauser *et al.* demonstrated a resonant PTE membrane with spectrally selective absorption [3]. Here, we report a narrowband PTE detector, which integrates a guided-mode resonance (GMR) filter and a thin-film thermocouple. The GMR-based PTE device utilizes the metal thermocouple as one of the cladding layers. Owing to the GMR phenomenon, the metal-cladding GMR filter can absorb light in a narrow bandwidth [4]. The structure of a metal-cladding GMR filter can be engineered to obtain a strong absorption at the desired wavelength [5].

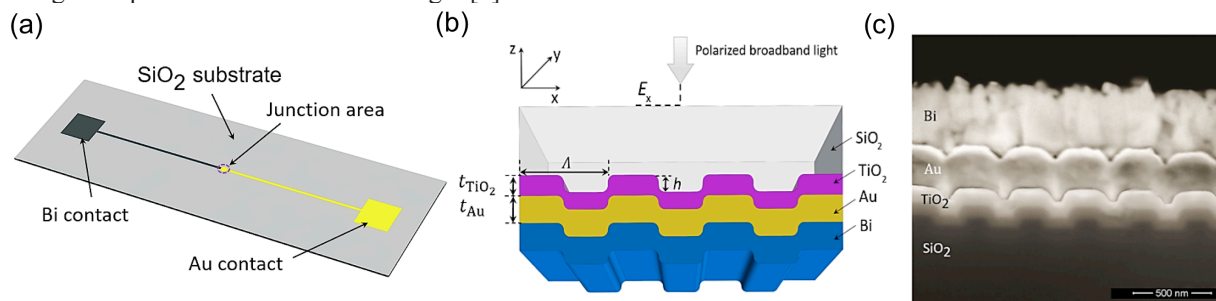


Fig. 1. Structure of the GMR-PTE detector. (a) Schematic diagram of the Au/Bi thermocouple on a glass slide. The GMR structure locates at the junction area. (b) Schematic diagram of the metal-cladding GMR filter excited by a linearly polarized light through the glass substrate. (c) Cross-sectional SEM image shows the stack of SiO₂/TiO₂/Au/Bi thin films.

The structure of the GMR-based narrowband PTE device is schematically shown in Fig. 1(a) and (b). The device consists of a one-dimensional GMR grating and a thin-film thermocouple. The thermocouple is formed at the junction between gold (Au) and bismuth (Bi) as shown in Fig. 1(a). The Au layer is in contact with the GMR grating and also functions as the metal cladding. The geometric parameters, including a period (Λ), grating depth (d), and waveguide thickness (t), can be designed to manifest a GMR resonance at the desired wavelength. In this work, the grating geometry is: $\Lambda = 360$ nm, duty cycle = 50%, and $d = 40$ nm. The grating structure was fabricated on a glass substrate using nanoimprint lithography [6]. A 100-nm film of titanium oxide (TiO₂) was evaporated onto the grating surface to act as the grating waveguide. Following the deposition of TiO₂, the 100-nm Au film and 200-nm Bi layer were deposited to produce the thermocouple with the output terminals as shown in Fig. 1(a). The SEM image in Fig. 1(c) illustrates the device structure in the vertical cross section. Illuminated through the glass substrate, the device can selectively absorb owing to the loss of the Au cladding. The absorption-induced temperature rises result in measurable voltage outputs of the Au/Bi thermocouple.

The GMR effect of the metal-cladding PTE device was modeled using the rigorous coupled-wave analysis and characterized experimentally. Simulation results of the PTE absorption are shown in Fig. 2. For normal incidence ($\theta = 0^\circ$), the device exhibits an absorption peak at $\lambda_r = 635$ nm with the full-width half-maximum (FWHM) of 20 nm and the absorption coefficient over 70% as shown in Fig. 2(a). Here, the excitation light is linearly polarized with the electric field parallel to the grating direction and metal surface (the y -axis defined in Fig. 1(b)). Since the excitation is

TE polarized, there is no surface plasmon resonance. At the resonance wavelength ($\lambda_r = 635$ nm), the local electrical field is significantly enhanced with regard to the incident light, as shown in Fig. 2(b). The enhanced near-field can facilitate the heat generation at the Au/Bi thermocouple. Absorption characteristics of the GMR-PTE device were experimentally measured using a broadband light source illuminated on the junction area for three different incident angles ($\theta = 0^\circ, 5^\circ,$ and 10°). The off-normal excitations exhibit two distinct absorption peaks (Fig. 3(a)).

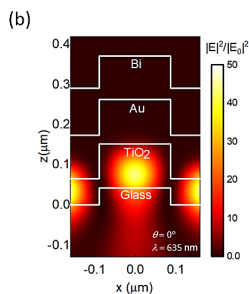
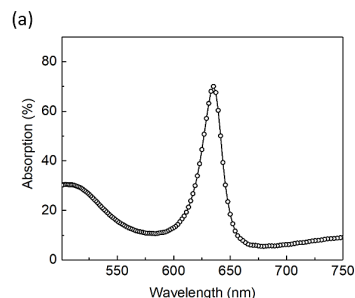


Fig. 2. Simulated absorption characteristics of the PTE device. (a) Absorption spectrum calculated for the normal incidence. (b) Calculated near-field distribution at the resonance condition within one period of the grating.

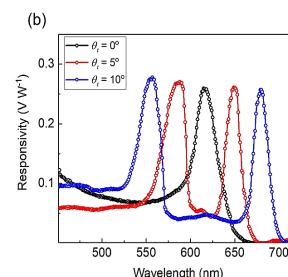
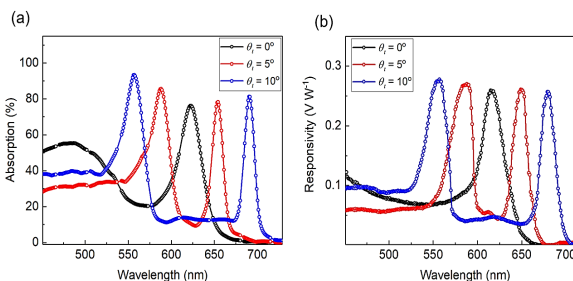


Fig. 3. Measured absorption spectra and voltage output of the PTE device. (a) Absorption spectra measured at $\theta = 0^\circ, 5^\circ,$ and 10° , respectively. (b) Voltage outputs of GMR-PTE as a function of wavelength measured at three different incident angles.

To investigate the narrowband PTE effect, we tested the device output when the junction area was illuminated by a narrowband excitation generated by a monochromator (Model 272, McPherson). The monochromator output was tuned from $\lambda = 450$ nm to 730 nm with the FWHM of 3 nm. The thermoelectric voltage (TEV) outputs were measured as a function of wavelength. The device responsivity was calculated by normalizing the TEV output using the power of incidence. Fig. 3(b) shows the responsivity spectra measured at three different angles ($\theta = 0^\circ, 5^\circ,$ and 10°). At $\theta = 0^\circ$, the peak of the responsivity locates at 617 nm with a FWHM of 30.5 nm. The wavelength-specific responsivity which can be adjusted by controlling the incident angle. For instance, at $\theta = 5^\circ$, two resonant peaks appear at 587 nm and 651 nm with FWHM of 18.9 nm and 27.5 nm, respectively. The device responsivity curves match well with the absorption spectra shown in Fig. 3(a).

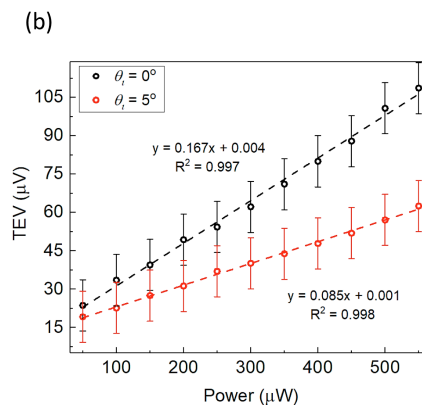
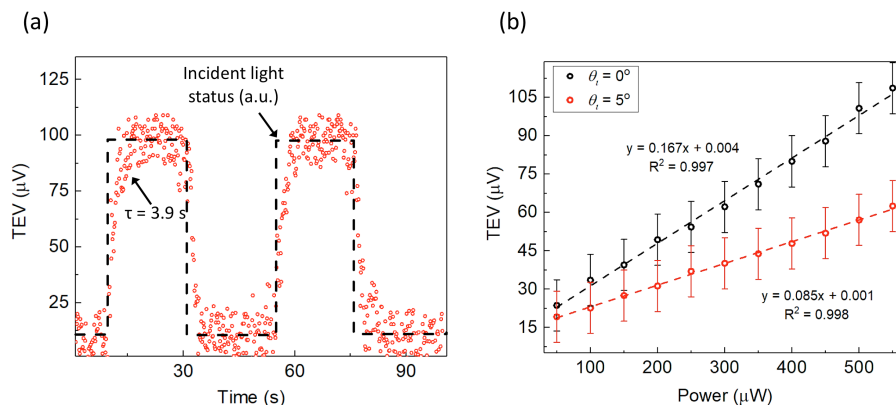


Fig. 4. Voltage output of the GMR-PTE device. (a) Dynamic TEV response of the PTE device for two consecutive heating/cooling cycles. The excitation wavelength is 617 nm. (b) TEV response as a function of incidence power.

The dynamic response of the PTE device was also studied. The PTE outputs during two heating/cooling cycles were measured as shown in Fig. 4(a). The rise time of the TEV response was approximately 3.9 s when the device was excited at $\lambda_r = 617$ nm and $\theta = 0^\circ$. Fig. 4(a) shows the TEV outputs as a function of incidence power measured at on resonance ($\theta = 0^\circ$) and off resonance ($\theta = 5^\circ$) conditions.

References

- [1] D. Dadarlat, P. R. N. Misse, A. Maignan, E. Guilmeau, M. Depriester, M. Kuriakose, A. Hadj Sahraoui, *Proc. SPIE*, **9258** (2015).
- [2] X. Cai, A. B. Sushkov, R. J. Suess, M. M. Jadidi, G. S. Jenkins, L. O. Nyakiti, R. L. Myers-Ward, S. Li, J. Yan, D. K. Gaskill, T. E. Murphy, H. D. Drew, and M. S. Fuhrer, *Nat. Nanotechnol.*, **9**, 814-819 (2014).
- [3] K. Mauser, W. Kelly, S. Kim, S. Mitrovic, D. Fleischman, R. Pala, K. C. Schwab, and H. A. Atwater, *Nat. Nanotechnol.*, **12**, 770-775 (2017).
- [4] Y. Ding and R. Magnusson, *Opt. Express* **12**, 1885-1892 (2004).
- [5] J. -N. Liu, M. V. Schulmerich, R. Bhargava, and B. T. Cunningham, *Opt. Express* **19**, 24182-24197 (2011).
- [6] L. Liu, J. Zhang, M. A. Badshah, L. Dong, J. Li, S. -M. Kim, and M. Lu, *Sci. Rep.*, **6**, 22445 (2016).